ACS OMEGA

Article

Cite This: ACS Omega 2019, 4, 11408−11413

http://pubs.acs.org/journal/acsodf

Antenna-like Ring Structures via Self-Assembly of Octaphosphonate Tetraphenyl Porphyrin with Nucleobases

Mahmood D. Aljabri,[†] Ratan W. Jadhav,[‡] Mohammad Al Kobaisi,[§] Lathe A. Jones,[†] Sidhanath V. Bhosale,*[,∥] and Sheshanath V. Bhosale*[,‡]

[†]School of Science, RMIT University, GPO Box 2476, Melbourne, Victoria 3001, Australia

[‡]School of Chemical Sciences, Goa University, Taleigao Plateau, Goa 403206, India

[§]Department of Chemistry and Biotechnology, FSET, Swinburne University of Technology, Hawthorn, Victoria 3122, Australia

[∥]Polymers and Functional Materials Division and Academy of Scientific and Innovative Research (AcSIR), CSIR-Indian Institute of Chemical Technology, Hyderabad 500007, Telangana, India

Supporting Information

ABSTRACT: Supramolecular self-assembly of an octaphosphonate tetraphenyl porphyrin with three different nucleobases (adenine, cytosine, and thymine) was studied. Porphyrin **1** with 8 and 10 equiv of cytosine produces light-harvesting ring-like structures, that is, architectures similar to those observed in natural light-harvesting antenna. However, porphyrin assembled with adenine or thymine resulted in prisms and microrods, respectively. UV−vis absorption, fluorescence, and dynamic light scattering were used to determine the mode of aggregation in solution. Scanning electron microscopy and X-ray diffraction spectroscopy used to visualize the self-assembled nanostructures and their behavior in the solid state, respectively. Thus, we believe that this study may demonstrate a deeper understanding on how one needs to manipulate donor/acceptor subunits in supramolecular assemblies to construct artificial antenna architectures.

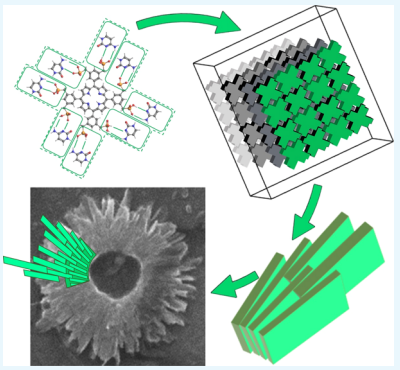

1. INTRODUCTION

The fabrication of highly ordered nanostructures of chromophores via self-assembly is an active area of research with diverse applications in materials science.[1] The evolutionary process in natural molecular structures such as a light-harvesting system employed in photosynthesis by purple bacteria and green plants constructed via self-assembly of chromophoric arrays has been used as inspiration.[2] In purple photosynthetic bacteria, the light-harvesting antenna systems LH1 and LH2 are created by the circular arrangement of chromophores and small biopolymers having ∼54 amino acids, which bind to Mg in BChl a.[2,3] X-ray crystal structure analyses of antenna systems have revealed the precise arrangement of pigments embedded in photosynthetic membranes and their position in proteins.[2,3b,c] More recently, atomic force microscopy studies have shown similar results.[3a] The chromophore pigments are tightly held by protein scaffolds at precise intermolecular distances to control the energy and electron transfer.[4] The absorption of light by the photosynthetic reaction centers stabilizes an exciton, which consists of an electron and a hole pair, on opposite sides of the photosynthetic membrane.[5] In the photosynthetic light-harvesting antenna systems LH1 and LH2, the chromophoric pigment arrays are organized in ring-shaped nanostructures.[6]

Researchers have attempted to use the natural photosynthetic system as a blueprint to fabricate artificial photosystems that can capture light efficiently.[7] It is not necessary to identically reproduce the natural system to achieve large-scale photosynthetic devices, even though polypeptides with ∼54 amino acids are synthetically feasible. To construct ring-shaped ordered arrays of pigments, most of the artificial photosynthetic antenna systems have been created via covalent bond forming synthetic procedures.[8] The creation of functional artificial antenna systems via self-assembly of pigments by noncovalent interactions utilizing H-bonding, hydrophobic, dipole-dipole, van der Waals interaction, $\pi-\pi$ stacking, and solvophobic effects is a desirable alternative approach.[9] To achieve the precise arrangement of the monomers in a dynamic and thermodynamically stable antenna system, the careful design of the chromophore pigments with specific molecular recognition sites are required.

Nolte and coworkers have shown that "ring-like" porphyrin based arrays can form by the evaporation of organic solutions containing molecular precursors on a substrate.[10] They presume that formation of ring-like structures is driven by evaporation of the solvent and its wetting/nonwetting characteristics. The self-assembly of $TPPS_4$ porphyrin into wheel-like structures was reported in 2005 by Rodaite et al.[11] Kobuke et al. have shown that a zinc-containing porphyrin with imidazole as a molecular recognition site yields stable

Received: April 1, 2019
Accepted: June 20, 2019
Published: July 1, 2019

DOI: 10.1021/acsomega.9b00909
ACS Omega 2019, 4, 11408−11413

macrocyclic arrays.[12] The same group further reported a macromolecular complex, containing 30 porphyrins bridged with ferrocene, that is, 10.5 nm in diameter when imaged on an Au(111) surface by using low-temperature ultrahigh-vacuum scanning tunneling microscopy.[13] The hexamer and dodecamer porphyrin arrays self-assemble into macrometer-sized ring structures, with evaporation of the solvent on the surface and assembly driven by a "pinhole" mechanism.[14] The supramolecular self-assembly of TPE-based porphyrins into ring-like structures via solvophobic control was reported in 2015 by our group.[15] In 2016, Balaban et al. have shown that solvent composition plays an important role to switch the assembly of porphyrin−phenylalanine−phenylalanine conjugates into fibrils, platelets, and nanospheres.[16] Very recently, Iida et al. have demonstrated the self-assembly of porphyrin containing macroscopic anisotropic structures by a light-induced solvothermal assembly.[17] Nucleobases are important building blocks present as subunits in biomacromolecules such as DNA and RNAs, among them pyrimidine and purines are involved in the formation of the DNA double helix structure via H-bonding,[18] and have been employed to fabricate functional materials.[19]

Recently, we reported on the formation of nanowires, nanorods, spherical, and chiral assemblies from octaphosphonate-tetraphenyl-porphyrin **1** with or without guest molecules.[20,21] In this manuscript, we present the self-assembly of porphyrin **1** with the nucleobase cytosine (C) at a range of molecular ratios (Figure 1). We found that cytosine triggered

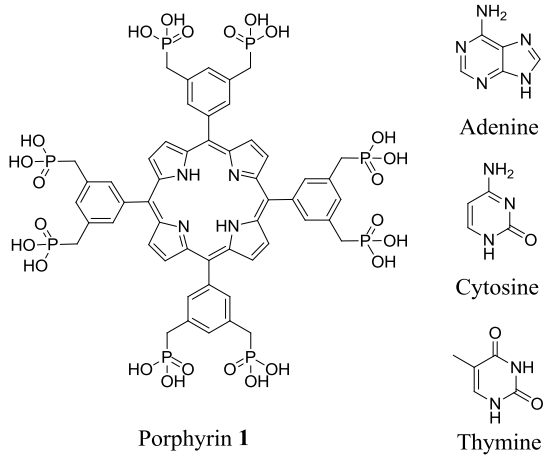

Figure 1. Molecular structures of octaphosphonate tetraphenyl porphyrin (**1**) and the three nucleic bases used in this study.

the assembly of porphyrin **1** into a light-harvesting antenna-like ring system at molecular ratios between 1 and 8. In contrast, in the presence of adenine (A) or thymine (Th), porphyrin **1** self-assembled into the prism and microrod morphologies, respectively.

2. RESULTS AND DISCUSSION

2.1. UV−Vis Absorbance Spectroscopy. The UV−vis absorbance spectrum of porphyrin **1** in water shows Soret band maxima at 440 nm with a shoulder peak at 418 nm along with four weak Q-bands at 516, 558, 602, and 660 nm (Figure 2a).[20] Typically, tetraphenyl-porphyrin[15] is known to absorb in the region around 420 nm, however, the large red-shift of **1** is perhaps attributed to the protonation of porphyrin by the phosphonate groups.[20] This is more evident upon the addition

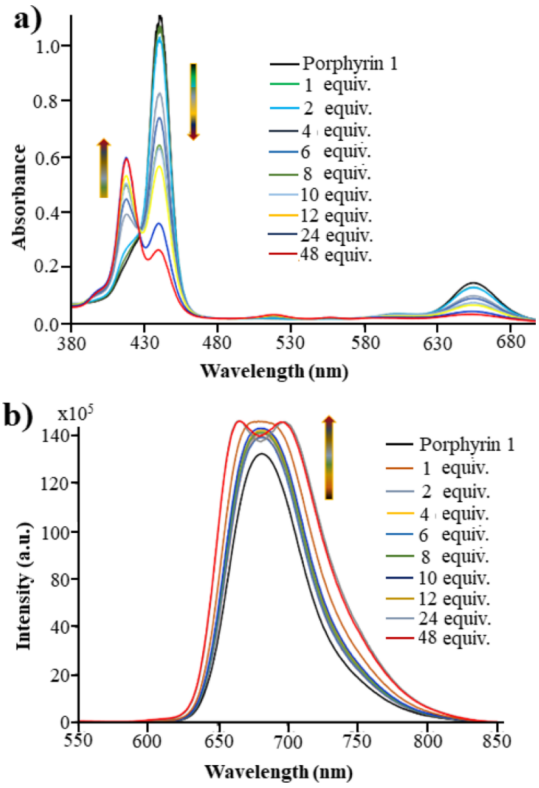

Figure 2. (a) UV−vis absorbance, (b) and emission spectrums of porphyrin **1** (1×10^{-4} M), and porphyrin **1**: cytosine at molecular ratios between 1:0 and 1:48 equiv.

of cytosine as a guest molecule. The UV−vis spectra of porphyrin **1** during titration with cytosine are shown in Figure 2a. The titration reveals significant changes in absorbance, indicative of an interaction between the analyte and the chromophore. No significant change in absorbance peaks was detected at 1 and 2 equiv of cytosine. However further incremental additions of cytosine from 4 to 48 equiv led to a decrease in both the Soret band at 440 nm and the Q-band at 660 nm, while the intensity of the shoulder peak at 418 nm increased. These changes in the absorbance spectra can be attributed to H-bonding between porphyrin phosphonic acid and cytosine, which is acting as the base. At 48 equiv of cytosine, the absorbance maxima at 440, 418, and 660 nm are saturated. The decrease in peak intensity at 440 nm and increase in peak intensity at 418 nm led to an isosbestic point at 429 nm, suggesting the presence of two species in solution.

In order to confirm the strong interaction of porphyrin **1** with cytosine, we have compared with other nucleobases such as (uracil, guanine, thymine, and adenine). However, a clear interaction and novel morphologies were observed with cytosine and we have not observed a marked interaction in the case of other tested nucleobases as shown in the Supporting Information Figures S1 and S2. Such a comparison could give clear evidence of the exclusive interaction of cytosine with porphyrin **1**. The incremental addition of A and Th led to no significant changes in the UV−vis absorbance spectra of porphyrin **1**. Figure S1a,b show the UV−vis absorbance spectra of porphyrin **1** with the addition of A and Th (0−48 equiv). With the addition of A or Th, the absorbance maxima of porphyrin **1** at 440 nm, the shoulder peak at 418 nm and the intense Q-band at 660 nm showed a 30% decrease in peak intensities (Figure S1a). These results

DOI: 10.1021/acsomega.9b00909
ACS Omega 2019, 4, 11408−11413

suggest that the aggregation of porphyrin **1** with A and Th proceeds via a different mode. Hereafter, the mode of aggregation of cytosine with porphyrin **1** is discussed in detail. In addition, the changes in electronic absorption spectra and an obvious blue shift in the absorbance spectra upon the addition of cytosine is attributed to the self-assembled nanostructure through place via H-type aggregates (opposite phenomenon to J-aggregates)[22] along with strong H-bonding between phosphonic acid of porphyrin and the amino functional group of cytosine.

2.2. Fluorescence Spectroscopy. The fluorescence emission spectra of porphyrin **1** in the presence of the nucleobases (C, A, and Th) was also examined in water (Figure 2b, and Supporting Information Figure S2a,b). The fluorescence spectrum of porphyrin **1** exhibits an emission band at 680 nm when excited at 418 nm. The emission spectra of porphyrin **1**: cytosine at 0−48 equiv is shown in Figure 2b. In the presence of 1 equiv of cytosine, the emission peak intensity of porphyrin **1** increased. With further incremental addition of cytosine (2−12 equiv), the emission spectra displayed an increase in quantum yield. The quantum yield of porphyrin **1** in the protonated form was shown to be 0.10, which is comparable to standard reference tetraphenylporphyrin (Φ_F = 0.11).[22] Interestingly, porphyrin **1** in the presence of 8 equiv of cytosine gives Φ_F = 0.21 and 10 equiv gives Φ_F = 0.23. With the further addition of cytosine (24 and 48 equiv), the emission peak of porphyrin **1** split into two peaks at 660 and 720 nm, this split of fluorescence emission was upon self-assembly there is limited electronic communication between porphyrin cores because of the network of H-bonding through adding excess of cytosine (Figure 2b).

We contrasted the self-assembly behavior of A and Th with porphyrin **1** compared with C in solution, and the fluorescence spectra of porphyrin **1** titrated with A and Th show similar behavior to C during titration (Figure S2a,b). We extended the examination of fluorescent emission of porphyrin **1** via titration with a common base, that is, triethylamine (Figure S2c). It can be clearly seen that upon incremental addition of trimethylamine (0−48 equiv) decreasing fluorescence emission was observed, it was probably due to deprotonation of porphyrin **1** and this behavior is the complete opposite to the self-assembly of porphyrin **1** in the presence of nucleobases (Figure 2b).

2.3. Scanning Electron Microscopy. Scanning electron microscopy (SEM) was used to investigate the morphology of microstructures of the self-assembled porphyrin **1**−cytosine with 1:1, 1:2, and 1:4 molecular ratios deposited on a silicon wafer by solvent evaporation, shown in Figures S3−S5 with the mechanism details described. Compound **1**−cytosine self-assembled into microflower-like structures. These fractal structures ranged between 5 and 10 μm in diameter.

Increasing the molecular ratios porphyrin **1**−cytosine to 8 equiv of cytosine gave a wheel-like circular arrangement after solvent evaporation (Figure 3a). The wheel-like arrangement grew larger and more defined at a 1:10 molecular ratio (Figure 3b). At 1:8 and 1:10 porphyrin **1**−cytosine molecular ratios fractal structures also were seen coexisting with the wheel-like circular microstructures (Figure S6). Their average wheel diameter was approximately 5 μm at 1:8 and 10 μm at 1:10 porphyrin **1**−cytosine self-assemblies (Figure 3c,d), respectively. The wheel-like arrangement appears to be composed of nanocrystallites stacked radially to form a hole in the middle. The inner diameter of the hole is approximately 2−4 μm.

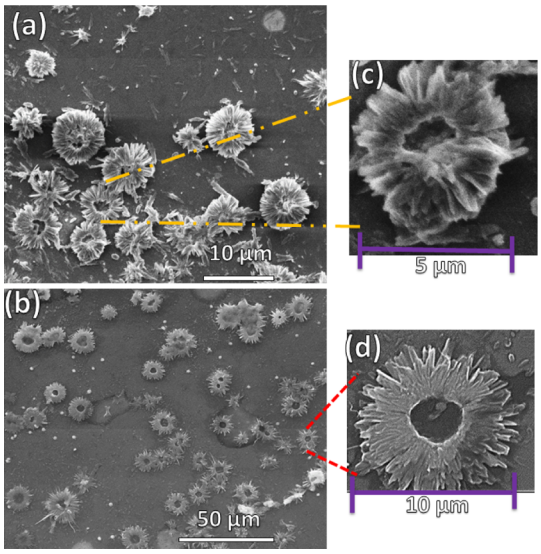

Figure 3. SEM micrographs of the supramolecular self-assembly of porphyrin **1** (1×10^{-4} M) in the presence of various ratios of cytosine: (a,c) 8 and (b,d) 10 equiv after solvent evaporation on a silicon wafer. The noncovalent acid−base interactions between porphyrin **1** and cytosine produces ring-like structures.

SEM was also used to investigate the morphology of microstructures of the self-assembled porphyrin **1**−cytosine with 1:1, 1:2, and 1:4 molecular ratios deposited on a silicon wafer by solvent evaporation, shown in Figure 4 with the mechanism details described. Compound **1**−cytosine self-assembled into microflower-like structures. These fractal

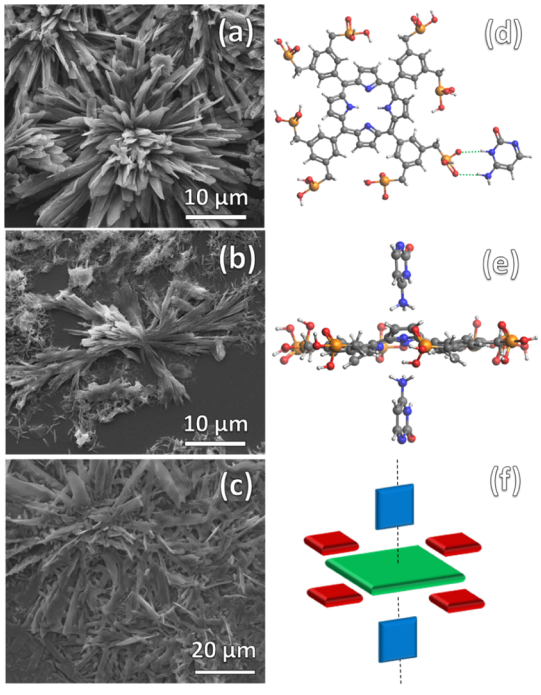

Figure 4. SEM micrographs of the supramolecular self-assembly of porphyrin **1** (1×10^{-4} M) and cytosine at (a) 1:1, (b) 1:2, and (c) 1:4 molecular ratios. Noncovalent acid−base interactions between porphyrin **1** and cytosine (d) in plane via phosphonate groups, and (e) in the axial position via the acidic pyrrole subunits of the porphyrin core. (f) Coordination scheme of cytosine−porphyrin **1** in the molecular plane and axial positions.

DOI: 10.1021/acsomega.9b00909
ACS Omega 2019, 4, 11408−11413

structures ranged between 5 and 10 μm in diameter. As a base, cytosine probes porphyrin **1** for the best position of interaction to form the most stable noncovalent acid−base bond. Porphyrin **1** possessed two acidic positions; the phosphonic groups with pK_{a_1} = 3.0, and the acidic pyrrole subunits of the porphyrin core with pK_{a_2} = 5.6, while the second phosphoric proton had a pK_{a_3} = 8.0. Therefore, cytosine coordinates with the phosphonic acid moieties of the porphyrin **1** molecule vis two H-bonds as shown in Figure 4d. The 8 peripheral phosphonic acid moieties are first consumed to form the in-plane complex. Beyond the 1:8 coordination, cytosine starts taking the axial position where the pyrrole subunits are deprotonated and the porphyrin core interacts with cytosine electrostatically, which is based on their acidic and basic properties, respectively.[23]

In order to gain an insight into the nucleobase-triggered supramolecular self-assembling behavior of porphyrin **1**, we also studied the assembly of A and Th. The results are presented in Figures S7 and S8, respectively. It was observed that in the presence of 10 equiv of A, porphyrin **1** was assembled into a microprism with a crystalline morphology of ∼5−8 μm size (Figure S7), while porphyrin **1** co-assembly with Th (10 equiv) produced microneedles tens of microns in length with up to a 10 μm square cross section (Figure S8).

2.4. X-ray Diffraction. X-ray diffraction (XRD) confirmed the crystallinity of porphyrin **1** upon self-assembly with C, A, and Th as shown in Figure S9. Porphyrin **1** did not exhibit any peak, confirming that the material does not crystalize alone. The XRD pattern of porphyrin **1** with cytosine at a 10 equiv molar ratio displays three peaks, a highly intense peak at 36° and a less intense peaks at 24° and 36°, indicating a crystalline structure in the aggregated state. It was observed that the XRD pattern of porphyrin **1** in the presence of A (10 equiv) shows an intense, sharp peak at 24° with two other less intense peaks at 20° and 35°, also suggesting crystalline morphology formation. Porphyrin **1** with the addition of Th resulted in two intense XRD pattern peaks at around 28° and 31°. These results indicate that in the presence of nucleobases C, A, and Th, porphyrin **1** undergoes different types of packing driven by different noncovalent interactions such as intermolecular H-bonding and porphyrin core stacking, leading to different types of morphology of porphyrin **1** in an aqueous medium. The high crystallinity evidenced by XRDs shows that the superstructures observed in SEM micrographs are composed of nano and microcrystalline self-assemblies. Dynamic light scattering (DLS) experiments were performed on the porphyrin **1** with various equivalents of cytosine (2, 4, 8, and 12 equiv) to confirm the size distribution of the assembled formation (Figure S10).

2.5. Proton NMR. The assembly formation upon addition of nucleobase C to the porphyrin **1** (4.39×10^{-3} M) was indicated by the shifting of signals in the ^{1}H NMR spectrum. With the addition of 1 equiv of C a marked upfield shift was observed for the aromatic proton of porphyrin **1**, moving from δ 8.35 to 8.24 ppm with broadening (Figure 5). For the incremental addition of C (2 and 10 equiv), upfield shifts of the aromatic proton signal to 8.15 and 8.03 ppm was observed, respectively. After addition of 8 equiv of C, the aromatic proton of porphyrin showed the appearance of a split proton peak at 8.02 and 7.99 ppm. In the presence of 10 equiv of C the NMR peaks of the porphyrin aromatic ring system appeared at 8.01 and 7.97 ppm. This particular signal

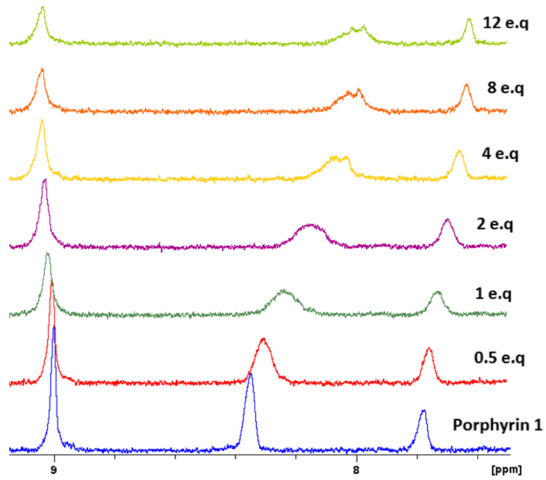

Figure 5. ^{1}H NMR spectrum of porphyrin **1** and with the addition of various equivalents (1−12) of cytosine in D_2O.

corresponds to payroll H_b of porphyrin **1**, indicating one recognition site of the molecule along with the phosphonate group. These ^{1}H NMR shifts of the proton peak indicate that H-bonding has taken place between porphyrin **1** and C via complementary molecular recognition sites. By observing all of these results, we interpret that the self-assembly takes place via intermolecular H-bonding, along with stacking of the porphyrin core, with the different interaction modes depending upon the ratio of C relative to the porphyrin **1**.

2.6. Schematic Representation of Molecular Co-Assembly. Up to a 1:8 ratio of porphyrin **1** to cytosine, the acid−base interaction results in a low charge density on both the weak acid and base molecular moieties, that is the phosphonic acid moieties and the amine functional group of the cytosine in the assembly, permitting the moderately hydrophobic core to self-assemble face to face in the aqueous environment. This leaves the peripheral phosphonate groups free to further grow in the porphyrin plane via interaction with cytosine. It is well known that the porphyrin self-assembly can result in multimeric ring structure antennas present in light harvesting systems. Similarly, ring-shaped superstructures were obtained at 1:8 and 1:10 porphyrin−cytosine ratios. The number of 1:8 complex porphyrin−cytosine subunits in such structures is dependent on the type and size of the moieties substituted on the porphyrin cores. Here, we have cytosine moieties extending the plane of the porphyrin core to give nanocrystalline subunits assembling in the ring shape, following the naturally occurring pattern at and around 1:8 porphyrin **1** to the cytosine ratio. Once this balance is disturbed the self-assembly results in radial fractal growth composed of crystalline blades (Figures 3 and S6a,c) and as graphically illustrated in Figure 6. These results are similar to the self-assembly of extended bodipy-derived π-conjugated systems,[24] which is a key player for nanoarchitectonics supramolecular materials.[25]

3. CONCLUSIONS

In summary, the supramolecular self-assembly of octaphosphonate tetraphenyl porphyrin **1** with three different nucleic bases [adenine (A), cytosine (C), and thymine (Th)] was studied. Porphyrin **1** assembled with C (1, 2 and 4 equiv) to produce microflowers and nanorods on a silicon wafer surface. The self-assembly of porphyrin **1** in the presence of 8/10 equiv

DOI: 10.1021/acsomega.9b00909
ACS Omega 2019, 4, 11408−11413

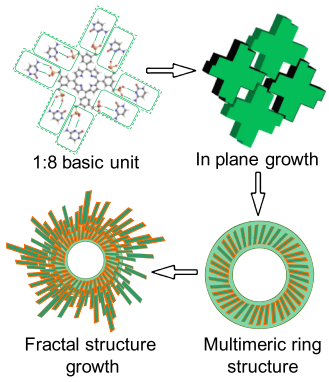

Figure 6. Schematic representation of molecular co-assembly of porphyrin **1** and cytosine above 1:8 molecular ratios.

of C yields well-defined ring-like structures similar to natural light-harvesting antennae. Furthermore, the co-assembled porphyrin with nucleobases A and Th exhibited prism and microrod-like structures, respectively. The controlled porphyrin ring-like supramolecular self-assembly formation opens up a new way of creating porphyrin arrays, and this self-assembly approach could be useful to construct artificial antenna similar to natural light-harvesting systems by manipulating donor/acceptor subunits.

4. EXPERIMENTAL SECTION

4.1. Materials. All nucleobase chemicals that are involved in this investigation were purchased from Sigma-Aldrich and used as they are without further purification.

4.2. Scanning Electron Microscopy. The method involved in this study started by the preparation of 1×10^{-4} M of porphyrin 1 in water pH (7.0) followed by addition of nucleobases (A, C, and Th) separately. From the resulting solution was added drop-wise into a silicon wafer which was slowly dried at room temperature and then coated with platinum before measurement.

■ ASSOCIATED CONTENT

Supporting Information

The Supporting Information is available free of charge on the ACS Publications website at DOI: 10.1021/acsomega.9b00909.

UV−vis absorbance, fluorescence, and SEM images and XRD and DLS analysis (PDF)

■ AUTHOR INFORMATION

Corresponding Authors

*E-mail: bhosale@iict.res.in (Sidhanath V. Bhosale).
*E-mail: svbhosale@unigoa.ac.in (Sheshanath V. Bhosale).

ORCID

Lathe A. Jones: 0000-0003-2498-2638
Sheshanath V. Bhosale: 0000-0003-0979-8250

Notes

The authors declare no competing financial interest.

■ ACKNOWLEDGMENTS

Sidhanath V. Bhosale (IICT) is grateful for the financial support from the SERB (DST) SB/S1/IC-009/2014, New Delhi, India and IICT/Pubs./2018/313. Sheshanath V. Bhosale (GU) acknowledges UGC-FRP for the financial support and Professorship. M.D.A. is thankful to Umm Al-Qura University for a full scholarship.

■ DEDICATION

This work is dedicated to Prof. B. R. Srinivasan and Prof. S. G. Tilve on the occasion of their 60th birthday.

■ REFERENCES

(1) (a) Sanders, J. K. M. *Comprehensive Supramolecular Chemistry*; Pergamon: New York, 1996; Vol. 9. (b) Kasha, M.; Rawls, H. R.; El-Bayoumi, M. A. The excitation model in molecular spectroscopy. *Pure Appl. Chem.* **1965**, *11*, 371−392. (c) Whitesides, G.; Mathias, J.; Seto, C. Molecular self-assembly and nanochemistry: a chemical strategy for the synthesis of nanostructures. *Science* **1991**, *254*, 1312−1319. (d) Kundu, S.; Patra, A. Nanoscale strategies for light harvesting. *Chem. Rev.* **2017**, *117*, 712−757. (e) Drain, C. M.; Varotto, A.; Radivojevic, I. Self-organized porphyrinic materials. *Chem. Rev.* **2009**, *109*, 1630−1658. (f) Lehn, J.-M. Toward self-organization and complex matter. *Science* **2002**, *295*, 2400−2403.

(2) McDermott, G.; Prince, S. M.; Freer, A. A.; Hawthornthwaite-Lawless, A. M.; Papiz, M. Z.; Cogdell, R. J.; Isaacs, N. W. Crystal-structure of an integral membrane light-harvesting complex from photosynthetic bacteria. *Nature* **1995**, *374*, 517−521.

(3) (a) Bahatyrova, S.; Frese, R. N.; Siebert, C. A.; Olsen, J. D.; van der Werf, K. O.; van Grondelle, R.; Niederman, R. A.; Bullough, P. A.; Otto, C.; Hunter, C. N. The native architecture of a photosynthetic membrane. *Nature* **2004**, *430*, 1058−1062. (b) Roszak, A. W.; Howard, T. D.; Southall, J.; Gardiner, A. T.; Law, C. J.; Isaacs, N. W.; Cogdell, R. J. Crystal structure of the RC-LH1 core complex from Rhodopseudomonas palustris. *Science* **2003**, *302*, 1969−1972. (c) Niwa, S.; Yu, L.-J.; Takeda, K.; Hirano, Y.; Kawakami, T.; Wang-Otomo, Z.-Y.; Miki, K. Structure of the LH1-RC complex from Thermochromatium tepidum at 3.0 Å. *Nature* **2014**, *508*, 228−232.

(4) (a) Pullerits, T.; Sundström, V. Photosynthetic light-harvesting pigment−protein complexes: toward understanding how and why. *Acc. Chem. Res.* **1996**, *29*, 381−389. (b) Balaban, T. S.; Braun, P.; Hättig, C.; Hellweg, A.; Kern, J.; Saenger, W.; Zouni, A. Preferential pathways for light-trapping involving beta-ligated chlorophylls. *Biochim. Biophys. Acta* **2009**, *1787*, 1254−1265.

(5) Linnanto, J.; Korppi-Tommola, J. E. I. Theoretical study of excitation transfer from modified B800 rings of the LH II antenna complex of Rps. acidophila. *Phys. Chem. Chem. Phys.* **2002**, *4*, 3453−3460.

(6) Bahatyrova, S.; Frese, R. N.; Van Der Werf, K. O.; Otto, C.; Hunter, C. N.; Olsen, J. D. Flexibility and Size Heterogeneity of the LH1 Light Harvesting Complex Revealed by Atomic Force Microscopy. *J. Biol. Chem.* **2004**, *279*, 21327−21333.

(7) (a) Barber, J.; Andersson, B. Revealing the blueprint of photosynthesis. *Nature* **1994**, *370*, 31−34. (b) Reddy, K. R.; Jiang, J.; Krayer, M.; Harris, M. A.; Springer, J. W.; Yang, E.; Jiao, J.; Niedzwiedzki, D. M.; Pandithavidana, D.; Parkes-Loach, P. S.; Kirmaier, C.; Loach, P. A.; Bocian, D. F.; Holten, D.; Lindsey, J. S. Palette of lipophilic bioconjugatable bacteriochlorins for construction of biohybrid light-harvesting architectures. *Chem. Sci.* **2013**, *4*, 2036−2053.

(8) (a) Grimsdale, A. C.; Müllen, K. The chemistry of organic nanomaterials. *Angew. Chem., Int. Ed.* **2005**, *44*, 5592−5629. (b) Burrell, A. K.; Officer, D. L.; Plieger, P. G.; Reid, D. C. W. Synthetic routes to multiporphyrin arrays. *Chem. Rev.* **2001**, *101*, 2751−2796. (c) Kim, D.; Osuka, A. Directly linked porphyrin arrays with tunable excitonic interactions. *Acc. Chem. Res.* **2004**, *37*, 735−745. (d) Satake, A.; Kobuke, Y. Dynamic supramolecular porphyrin systems. *Tetrahedron* **2005**, *61*, 13−41. (e) Uetomo, A.; Kozaki, M.; Suzuki, S.; Yamanaka, K.-I.; Ito, O.; Okada, K. Efficient light-harvesting antenna with a multi-porphyrin cascade. *J. Am. Chem. Soc.* **2011**, *133*, 13276−13279.

(9) (a) Frischmann, P. D.; Mahata, K.; Würthner, F. Powering the future of molecular artificial photosynthesis with light-harvesting

DOI: 10.1021/acsomega.9b00909
ACS Omega 2019, 4, 11408−11413

metallosupramolecular dye assemblies. *Chem. Soc. Rev.* **2013**, *42*, 1847−1870. (b) Elemans, J. A. A. W.; van Hameren, R.; Nolte, R. J. M.; Rowan, A. E. Molecular materials by self-assembly of porphyrins, phthalocyanines, and perylenes. *Adv. Mater.* **2006**, *18*, 1251−1266.

(10) (a) Schenning, A. P. H. J.; Benneker, F. B. G.; Geurts, H. P. M.; Liu, X. Y.; Nolte, R. J. M. Porphyrin wheels. *J. Am. Chem. Soc.* **1996**, *118*, 8549−8552. (b) Latterini, L.; Blossey, R.; Hofkens, J.; Vanoppen, P.; De Schryver, F. C.; Rowan, A. E.; Nolte, R. J. M. Ring formation in evaporating porphyrin derivative solutions. *Langmuir* **1999**, *15*, 3582−3588.

(11) Snitka, V.; Rackaitis, M.; Rodaite, R. Assemblies of TPPS4 porphyrin investigated by TEM, SPM and UV−vis spectroscopy. *Sens. Actuators, B* **2005**, *109*, 159−166.

(12) Kuramochi, Y.; Satake, A.; Kobuke, Y. Light-harvesting macroring accommodating a tetrapodal ligand based on complementary and cooperative coordinations. *J. Am. Chem. Soc.* **2004**, *126*, 8668−8669.

(13) Shoji, O.; Tanaka, H.; Kawai, T.; Kobuke, Y. Single molecule visualization of coordination-assembled porphyrin macrocycles reinforced with covalent linkings. *J. Am. Chem. Soc.* **2005**, *127*, 8598−8599.

(14) (a) Lensen, M. C.; Takazawa, K.; Elemans, J. A. A. W.; Jeukens, C. R. L. P. N.; Christianen, P. C. M.; Maan, J. C.; Rowan, A. E.; Nolte, R. J. M. Aided self-assembly of porphyrin nanoaggregates into ring-shaped architectures. *Chem.—Eur. J.* **2004**, *10*, 831−839. (b) Jeukens, C. R. L. P. N.; Lensen, M. C.; Wijnen, F. J. P.; Elemans, J. A. A. W.; Christianen, P. C. M.; Rowan, A. E.; Gerritsen, J. W.; Nolte, R. J. M.; Maan, J. C. Polarized absorption and emission of ordered self-assembled porphyrin rings. *Nano Lett.* **2004**, *4*, 1401−1406.

(15) Rananaware, A.; Bhosale, R. S.; Ohkubo, K.; Patil, H.; Jones, L. A.; Jackson, S. L.; Fukuzumi, S.; Bhosale, S. V.; Bhosale, S. V. Tetraphenylethene-based star shaped porphyrins: synthesis, self-assembly, and optical and photophysical study. *J. Org. Chem.* **2015**, *80*, 3832−3840.

(16) Charalambidis, G.; Georgilis, E.; Panda, M. K.; Anson, C. E.; Powell, A. K.; Doyle, S.; Moss, D.; Jochum, T.; Horton, P. N.; Coles, S. J.; Linares, M.; Beljonne, D.; Naubron, J.-V.; Conradt, J.; Kalt, H.; Mitraki, A.; Coutsolelos, A. G.; Balaban, T. S. A switchable self-assembling and disassembling chiral system based on a porphyrin-substituted phenylalanine−phenylalanine motif. *Nat. Commun.* **2016**, *7*, 12657.

(17) Yamamoto, Y.; Nishimura, Y.; Tokonami, S.; Fukui, N.; Tanaka, T.; Osuka, A.; Yorimitsu, H.; Iida, T. Macroscopically anisotropic structures produced by light-induced solvothermal assembly of porphyrin dimers. *Sci. Rep.* **2018**, *8*, 11108.

(18) Sivakova, S.; Rowan, S. J. Nucleobases as supramolecular motifs. *Chem. Soc. Rev.* **2005**, *34*, 9−21.

(19) Pu, F.; Ren, J.; Qu, X. Nucleobases, nucleosides, and nucleotides: versatile biomolecules for generating functional nanomaterials. *Chem. Soc. Rev.* **2018**, *47*, 1285−1306.

(20) (a) Bhosale, S. V.; Kalyankar, M. B.; Langford, S. J.; Bhosale, S. V.; Oliver, R. F. Synthesis and supramolecular properties of a novel octaphosphonate porphyrin. *Eur. J. Org. Chem.* **2009**, 4128−4134. (b) Bhosale, S. V.; Kalyankar, M. B.; Nalage, S. V.; Lalander, C. H.; Bhosale, S. V.; Langford, S. J.; Oliver, R. F. pH dependent molecular self-assembly of octaphosphonate porphyrin of nanoscale dimensions: nanosphere and nanorod aggregates. *Int. J. Mol. Sci.* **2011**, *12*, 1464−1473. (c) Bhosale, R. S.; La, D. D.; Al Kobaisi, M.; Bhosale, S. V.; Bhosale, S. V. Melamine and spermine mediated supramolecular self−assembly of octaphosphonate tetraphenyl porphyrin. *ChemistrySelect* **2017**, *2*, 1573−1577. (d) Rananaware, A.; La, D. D.; Al Kobaisi, M.; Bhosale, R. S.; Bhosale, S. V.; Bhosale, S. V. Controlled chiral supramolecular assemblies of water soluble achiral porphyrins induced by chiral counterions. *Chem. Commun.* **2016**, *52*, 10253−10256.

(21) Bricks, J. L.; Slominskii, Y. L.; Panas, I. D.; Demchenko, A. P. Fluorescent J-aggregates of cyanine dyes: basic research and applications review. *Methods Appl. Fluoresc.* **2017**, *6*, 012001.

(22) Seybold, P. G.; Gouterman, M. Porphyrins. *J. Mol. Spectrosc.* **1969**, *31*, 1−13.

(23) Bhosale, S. V.; Kalyankar, M. B.; Nalage, S. V.; Lalander, C. H.; Bhosale, S. V.; Langford, S. J.; Oliver, R. F. pH Dependent Molecular Self-Assembly of Octaphosphonate Porphyrin of Nanoscale Dimensions: Nanosphere and Nanorod Aggregates. *Int. J. Mol. Sci.* **2011**, *12*, 1464−1473.

(24) (24) Ariga, K.; Nishikawa, M.; Mori, T.; Takeya, J.; Shrestha, L. K.; Hill, J. P. Self-assembly as a key player for materials nanoarchitectonics. *Sci. Technol. Adv. Mater.* **2019**, *20*, 51−95.

(25) Cherumukkil, S.; Vedhanarayanan, B.; Das, G.; Praveen, V. K.; Ajayaghosh, A. Self-Assembly of Bodipy-Derived Extended π-Systems. *Bull. Chem. Soc. Jpn.* **2018**, *91*, 100−120.

DOI: 10.1021/acsomega.9b00909
ACS Omega 2019, 4, 11408−11413